

Title No. 120-M23

Durability Aspects of Concrete Containing Nano-Titanium Dioxide

by Garima Rawat, Sumit Gandhi, and Yogesh Iyer Murthy

The current paper investigates the effects of partial cement replacement with nano-titanium dioxide (nano-TiO₂ [NT]) in varying weight proportions in concrete. In the C20/25 grade of concrete, NT was added by weight of cement with partial replacement of 0, 0.5, 1.5, 2.0, 2.5, and 3.0% using portland pozzolana cement. The physical and mechanical properties of the resulting concrete were assessed, as well as aspects of durability such as sorptivity and nondestructive tests (NDT) such as ultrasonic pulse velocity (UPV). Compared with the control mixture, the fresh concrete produced showed a drastic reduction in slump with increasing percentage of replacement, with a 54% reduction at a 3.0% replacement. Furthermore, for 1.5% NT, the compressive, flexural, and splitting tensile strengths peaked at 7, 28, 56, and 90 days, after which the values decreased. The addition of NT improved the homogeneity and integrity of the resulting concrete based on the UPV values. As the percentage of NT increased, chloride penetration decreased. From microstructural studies, it can be concluded that NT acts as a filler material and can be used as a partial replacement for cement in concrete up to 2% by weight.

Keywords: chloride penetration; durability; mechanical properties; nano-titanium dioxide (nano-TiO₂ [NT]); slump.

INTRODUCTION

The use of concrete in buildings and construction may have begun a century ago. However, as the use of concrete has increased from decade to decade, extensive and effective research has been conducted on improving concrete properties by incorporating a wide range of supplementary cementitious materials such as pozzolans and nanoparticles.¹ The addition of fine fillers has been shown to alter the initial hydration reaction, setting time, dimensional stability, and strength development of cement.² Owing to the growing interest in inert additives to cement, such as nano-titanium dioxide (nano-TiO₂ [NT]), a study focusing exclusively on the effects of chemically inert fillers on cement hydration is required.³ In recent years, nanoparticles have received much attention, and their various forms have been shown to be very useful in enabling the development of stronger and more durable concrete with better mechanical properties.⁴

NT is one of the most commonly used nano-additives in cement-based materials.^{3,4} Titanium dioxide is a noncombustible, odorless powder that has been widely produced and used in a variety of applications⁵ because of its high chemical stability, nontoxicity, anticorrosion, electrical, and superior photocatalytic properties.⁶ It exists in three stages: brookite, rutile, and anatase.⁷ Although the majority of TiO₂ used to date has not been nanosized, the use of titania nanoparticles has increased significantly and is expected to surpass the use

of conventional titanium dioxide in the coming years.⁸ When compared to conventional TiO₂, NT has a 500% increase in the surface area.⁹ It is also available in extremely pure form (99.9%).

Several researchers^{5,6,10} have developed cement-based or asphalt-based concrete that incorporates TiO₂ nanoparticles to increase its durability or impart certain desirable properties. Due to its chemical stability, high catalytic activity, and low cost, the incorporation of NT into cement-based materials has garnered considerable interest.⁸ However, its effects on the properties of cement-based materials are far from satisfactory.

Due to the strong binding property of cementitious materials, NT can be used in these materials without any additional processing.⁸ In addition, hardened mortars/concretes have porous structures that are ideal for the adsorption of NT particles. The three most common forms of titanium dioxide are rutile, anatase, and brookite. Titanium dioxide is also referred to as self-cleaning concrete or white concrete.¹¹ It not only ensures the structural integrity of the structures, but also their aesthetic appearance.

According to some reports,^{12,13} NT can extend the service life of cement-based materials and thus their construction, resulting in long-term economic benefits.

- Spurred by the increasing value of sustainability, there is a growing interest in TiO₂ use in construction materials to create photocatalytic coatings and materials.
- In the presence of near-ultraviolet (UV)/UV radiation ($h\nu$), oxygen, and water, a chain of photochemical surface reactions occur, which lead to strong oxidizing capability and which can oxidize NO_x (NO + NO₂), organic (volatile organic compounds [VOCs]), and inorganic compounds.
- The addition of NT provides a reduction in porosity, leading to pore structure refinement (smaller pores) while reducing clinker content.
- Strength is maintained while reducing clinker fraction; nanoparticles densify the paste structure.

Cementitious materials mixed with NT have the functions of air purification,¹¹ self-cleaning,⁸ and disinfection,¹⁴ which are the reasons for their wide application in the exterior

ACI Materials Journal, V. 120, No. 2, March 2023.

MS No. M-2022-067.R3, doi: 10.14359/51738490, received October 6, 2022, and reviewed under Institute publication policies. Copyright © 2023, American Concrete Institute. All rights reserved, including the making of copies unless permission is obtained from the copyright proprietors. Pertinent discussion including author's closure, if any, will be published ten months from this journal's date if the discussion is received within four months of the paper's print publication.

Table 1—Physical properties of OPC (Grade 53)

Fineness, %	Le Chatelier soundness, in. (mm)	Specific gravity	Consistency, seconds (minutes)	Setting time, seconds (minutes)		Compressive strength, psi (MPa)		
				Initial setting time	Final setting time	3 days	7 days	28 days
2.0	0.29 (7.5)	3.14	1800 (30)	6000 (100)	14,400 (240)	4206.09 (29)	5511.43 (38)	8412.18 (58)

surface of buildings including hospitals, restaurants, and airports.

There are few cases of nanoparticles being incorporated into cement-based concrete. Lee¹⁵ examined the characteristics of cement mortars containing nanoparticles to determine their super-mechanical and smart (temperature and strain-sensing) potentials. So far, however, research^{7,16} has mostly focused on establishing good mechanical performance with cement replacement materials at the microlevel.

Furthermore, despite being chemically inert in terms of its potential to directly react during cement hydration,^{12,13,17-19} NT can generally improve the mechanical performance and durability, as well as decrease the rigidity of cementitious materials.^{4,20-23} Moreover, the flexural fatigue performance and abrasion resistance of concretes were reported to be remarkably improved with the use of TiO₂ nanoparticles.²⁴ The gain in strength in this case might be related to the microstructural modification and the hydration acceleration effects of NT by providing additional surface area for product nucleation (that is, the boundary nucleation effect).^{19,24-27} The addition of TiO₂ nanoparticles leads to greater homogeneity, better compaction, and reduction in the pore volume and the pore size of cementitious materials, which results in a remarkable reduction in permeability.^{3,8,16,28,29} Titania nanoparticles have been also found to behave as an activator to accelerate the pozzolanic reaction, increase the rate of cement hydration, increase the intensity of the heat peak, and reduce the initial and final setting times and freezing-and-thawing damage. The mechanical properties were also enhanced with the use of NT. The addition of NT to cement-based materials can help them overcome some of their shortcomings, such as low tensile strength and resistance to harmful chemical penetration.

The effect of using NT in cementitious composites on their fresh properties, mechanical properties, and durability is demonstrated in this section.³⁰ In addition, the microstructural properties of nano-titania-incorporated mortar and concrete are investigated using scanning electron microscopy (SEM) images. Because the final performance of cementitious composites is directly related to their strength and permeability,³¹ this section will concentrate on the effect of NT on the mechanical properties and permeability of cement mortar and concrete.

RESEARCH SIGNIFICANCE

The effects of NT on the strength, durability, and microstructure of ordinary portland cement (OPC) are investigated in this paper. The compressive, splitting tensile, and flexural strengths were used to determine the mechanical properties. Water absorption, capillary absorption, and chloride penetration tests were used to determine the transport

Table 2—Chemical properties of OPC (Grade 53), %

Loss on ignition	CaO	SiO ₂	Al ₂ O ₃	Fe ₂ O ₃	MgO	K ₂ O	Na ₂ O
2.75	66.52	18.33	4.37	4.70	0.73	0.75	0.12

properties. The pore structure and microstructure of the concrete were examined using SEM. The sorptivity, chloride penetration, and ultrasonic pulse velocity (UPV) characteristics of endurance materials were investigated. The authors believe that this study will demonstrate that it is possible to obtain good-quality concrete at a slight cost increase by using novel materials.

Because NT improves the overall performance of cement-based materials, as well as their durability and sustainability, it reduces construction maintenance and repair costs. Furthermore, NT endows cement-based materials with new properties such as self-cleaning properties, resulting in lower routine cleaning and maintenance costs.²⁰ According to some reports,^{24,32,33} NT can extend the service life of cement-based materials and, as a result, constructions, resulting in long-term economic benefits.

EXPERIMENTAL PROCEDURE

Materials

The following materials were used in the experimental procedure. The materials, along with their physical and chemical properties, are given in the following tables.

Cement—OPC Grade 53 conforming to IS 12269:2013³⁴ was used in this work. The physical properties of the cement used in the construction of slabs are presented in Table 1.

The chemical properties following IS 12269:2013³⁴ were also evaluated and are presented in Table 2.

Aggregates—Basalt with a particle size of less than 20 mm that satisfied IS 2386-1963²⁵ was used. These were cleaned and dried in the open air for 24 hours after being thoroughly washed with tap water. Silt, dust, and unsound particles were removed from the concrete. The properties of the aggregates used are presented in Table 3.¹²

In this study, river sand that met the requirements of IS 383:2016³⁵ was employed for the particle-size distribution.

Water—All the concrete mixtures were mixed and cured with municipally supplied portable tap water that was free of organic contaminants, as proven by IS 456:2000³⁶ and IS 10500:2012.³⁷ Table 4 shows the qualities of the tap water.

TiO₂ nanoparticles—A company in India supplied the NT powder directly. The properties of the TiO₂ nanoparticles are provided in Table 5.

Mixture proportions and preparation of specimens

According to IS 10262:2019,³⁸ the nomenclature and proportions of the concrete mixtures are presented in Table 6.

The concrete was mixed using a pan mixer with a capacity of 26.41 gal. (100 L). The surface of all of the particles used in the concrete mixture was saturated and dry. All of the combinations were created by substituting cement in the following weight percentages: 0, 0.5, 1, 1.5, 2.0, 2.5, and 3.0%.

The dispersing agent sodium tripolyphosphate (STPP) for dispersing the nanoparticles, which works as a high-range water-reducing admixture (HRWRA) as well, was mixed with half the amount of water. The workability, strength, and durability of numerous concrete combinations were tested using cube, beam, and cylinder specimens. For curing, the test specimens were immersed in water at $80.6 \pm 3.6^\circ\text{F}$ ($27 \pm 2^\circ\text{C}$) until they achieved the testing age. Table 7 summarizes all of the experiments, including the specimen age,

specimen size, testing apparatus, and the standard code used throughout testing.

Testing methods

Compressive strength—Cubes sized 5.91 in. (150 mm) were made and evaluated at 7, 28, and 56 days after curing for the five different replacements under IS 516-1959.²⁶ A steady force of 458.87 kp/s (4.5 kN/s) was applied during compression testing until the cube disintegrated and no higher load could be sustained. After 28 days, SEM and energy-dispersive spectroscopy (EDS) investigations were conducted on the broken samples from each replacement.

Splitting tensile test—Splitting tensile tests were conducted following IS 5816:1999,⁴⁰ which required the preparation of 5.91 in. (150 mm) diameter and 11.81 in.

Table 3—Properties of coarse aggregate and fine aggregate conforming to IS 2386-1963 (Revision 2016)²⁵

Coarse aggregate			Fine aggregate		
S.No.	Property	Values	S.No.	Property	Values
1	Aggregate crushing value, %	19.62	1	Bulk density, kg/m ³	1582
2	Aggregate impact value, %	10.88	2	Fineness modulus	2.58
3	Los Angeles abrasion value, %	12.58	3	Water absorption, %	0.57
4	Bulk density, kg/m ³	1643	4	Specific gravity	2.63
5	Fineness modulus	6.35			
6	Water absorption, %	0.49			
7	Flakiness index, %	6.8			
8	Elongation index, %	11.8			
9	Specific gravity	2.68			

Table 4—Tap water characteristics

S.No.	Parameter	Value
1	Chloride	0.0014 lb/gal. (168 mg/L)
2	pH	7.6
3	Fluoride	0.000003 lb/gal. (0.4 mg/L)
4	Dissolved oxygen	0.00008 lb/gal. (10.15 mg/L)
5	Chemical oxygen demand	0
6	Biological oxygen demand	0
7	Free residual chlorine	8.34×10^{-7} lb/gal. (0.1 mg/L)

Table 5—Properties of TiO₂ nanoparticles

S.No.	Properties	Observed values
1	Type	TiO ₂ (rutile)
2	Diameter, in. (nm)	3.93×10^{-7} to 7.87×10^{-7} (10 to 20)
3	Surface volume ratio, m ² /g	163
4	Density, lb/in. ³ (g/cm ³)	0.135 (3.74)
5	Purity, %	>99.9%

Table 6—Nomenclature and mixture proportions of NT-added concrete

Concrete mixture nomenclature	Mixture proportions, lb/yd ³ (kg/m ³)					
	Cement replacement, %	Cement	Fine aggregate	Coarse aggregate	NT	Water
NT0	0	648.93 (385)	1172.42 (695.57)	1913.82 (1135.43)	0	323.62 (192)
NT0.5	0.5	645.68 (383.07)	1172.42 (695.57)	1913.82 (1135.43)	3.23 (1.92)	323.62 (192)
NT1	1	642.44 (381.15)	1172.42 (695.57)	1913.82 (1135.43)	6.48 (3.85)	323.62 (192)
NT1.5	1.5	639.21 (379.23)	1172.42 (695.57)	1913.82 (1135.43)	9.72 (5.77)	323.62 (192)
NT2	2	635.95 (377.30)	1172.42 (695.57)	1913.82 (1135.43)	12.97 (7.70)	323.62 (192)
NT2.5	2.5	632.70 (375.37)	1172.42 (695.57)	1913.82 (1135.43)	16.21 (9.62)	323.62 (192)
NT3	3	629.47 (373.45)	1172.42 (695.57)	1913.82 (1135.43)	19.46 (11.55)	323.62 (192)

Table 7—Details of experiments carried out

Test	Age of concrete, days	Specimen size, in. (mm)	Apparatus/instrument	Reference
Slump	Fresh concrete	—	Standard slump cone	IS 1199-1959 ³⁹
Compressive strength	7, 28, 56, and 90	5.9 x 5.9 x 5.9 (150 x 150 x 150) (cube)	Compression testing machine/universal testing machine	IS 516-1959 ²⁶
Splitting tensile strength	7, 28, 56, and 90	3.93 diameter and 7.87 height (100 diameter and 200 height) (cylinder)	Compression testing machine/universal testing machine	IS 5816:1999 ⁴⁰
Flexural strength	7, 28, 56, and 90	3.93 x 3.93 x 19.68 (100 x 100 x 500) (beam)	Flexure testing machine	IS 516-1959 ²⁶
Sorptivity	90	5.9 x 5.9 x 5.9 (150 x 150 x 150) (cube)	Weighing machine	—
Water absorption	28	5.9 diameter x 11.81 height (150 diameter x 300 height) (cylinder)	Extensometers	IS 516-1959 ²⁶
Scanning electron microscopy	28	Samples of SEM	Scanning electron microscope	—

(300 mm) height cylinders and their testing at 7, 28, and 56 days. The specimens were tested using universal testing equipment capable of withstanding a force of 203,943.2426 kip (2000 kN). Without using a shock, a steady load was introduced and gradually increased over time at a rate of 1.2 to 2.4 N/(mm²/min).

Flexural strength—According to Nazari,⁷ the specimens containing NT were tested for 28 days under four-point loads using flexural testing equipment. The experiment was conducted using a constant loading system with a shear span of 11.81 in. (300 mm) and a depth ratio of 3.0 for the shear span. Following production, the examples were positioned on the supporting bearing blocks with one side in proportion to the other. At a quarter distance from the ends of the supports, the upper surface of the test specimen was brought into contact with the load-applying block.⁴¹ The load-bearing block is brought into complete contact with the beam surface as a result of this technique. The beam was tested for uniform contact between the bearing and load-bearing blocks. The specimen was loaded repeatedly until it failed and the dial ceased to spin.⁴¹ The maximum applied load was indicated and recorded by the testing equipment. The following equation is used to determine the flexural strength

$$R = \frac{3FL}{4bd^2}$$

where *R* is the flexural strength in N/mm²; *F* is the applied load at failure; *L* is the beam span measured in mm; *b* is the beam breadth measured in mm; and *d* is the beam depth measured in mm.

Sorptivity—Three 30 mm slices were cut from three concrete cubes measuring 3.93 x 3.93 x 2.75 in. (100 x 100 x 70 mm) to conduct the sorptivity test.¹² These cubes have a life span of 90 days. The specimens were dried in an oven at a temperature of 131°F (55°C) for 3 days before being chilled in desiccators. Water absorption from the sides was blocked by coating the sidewalls with epoxy resin, allowing absorption only from the bottom. The specimens were immersed in tap water in pans with a water level of 0.19 in. (5 mm) above the pan’s bottom. The experimental

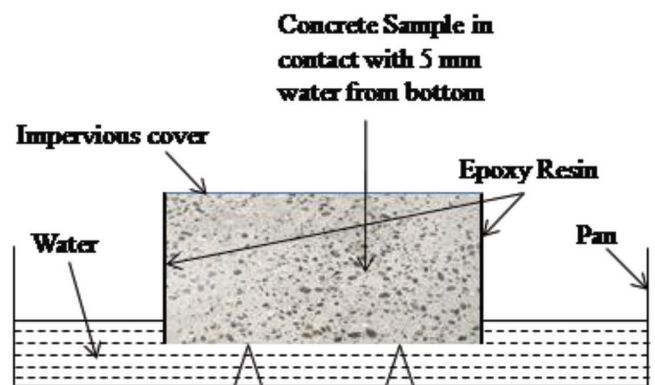


Fig. 1—Experimental setup for sorptivity measurements.

setup is depicted schematically in Fig. 1. After draining extra water with an absorbent cloth, the mass of these specimens was accurately determined at regular intervals. The slope of a line fitted to the plot of the cumulative absorbed volume of water per unit area of inflow surface versus the square root of time was obtained using data on the absorbed volume of water.⁴² The sorptivity coefficient is calculated using the following formula

$$f_{sc} = i/\sqrt{t}$$

where *f_{sc}* is the sorptivity coefficient in mm/√min; *i* is the cumulative absorbed volume of water per unit area of inflow surface in mm; and *t* is the elapsed time in minutes. For each test, the readings up to 960 seconds (16 minutes) were ignored to find the slope of the best-fit curve.

Characterization using SEM and EDS

The microstructure and morphology of NT concrete were investigated using EDS and SEM.^{3,12} After 28 days, the sample strength was determined and minute fragments of the core were removed. Before SEM analysis, the samples were placed in a desiccator and dried at 1472°F (800°C) overnight to remove moisture. Broken fragments from tested concrete specimens were mounted on brass stabs with carbon ribbons, gold-coated, and viewed under a scanning electron microscope for their microstructure.²⁷ The samples were analyzed

using a 78.74 in. (2 μm) diameter probe, a 15 kV accelerating voltage, and a 50 mA probe current. The SEM results are projected to be accurate to within a margin of error of $\pm 2\%$. Figure 2 shows the microstructure of the NT concrete.

RESULTS AND DISCUSSION

In this experimental program, the durability properties of the mixtures were measured by slump flow D (mm). Figure 3 presents the results of the tests performed on fresh concrete.

Slump flow

The fresh properties of all replacements are depicted in Fig. 3 (with and without NT). All of the concrete mixtures included the same quantity of water.²⁷ When NT was added to the concrete, it resulted in a new material that was hard but cohesive and sticky. As a result, the specimen workability decreased in direct proportion to the amount of cement replaced with NT. NT2, roughly 1.42 in. (36 mm), had the lowest slump value. NT has a limited lubricating effect and thus low workability due to its fast water absorption rate and low water content.⁴³ As a result of the mixing technique, the porous NT particles absorbed more water internally than the natural fine aggregate in the mixture. The rough texture and

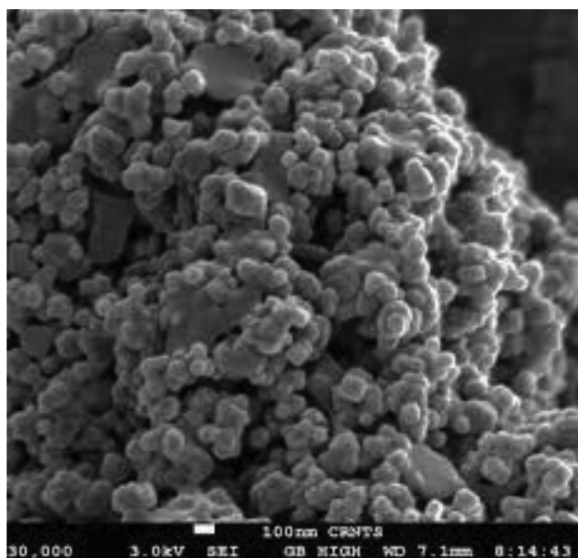


Fig. 2—Microstructure of NT.

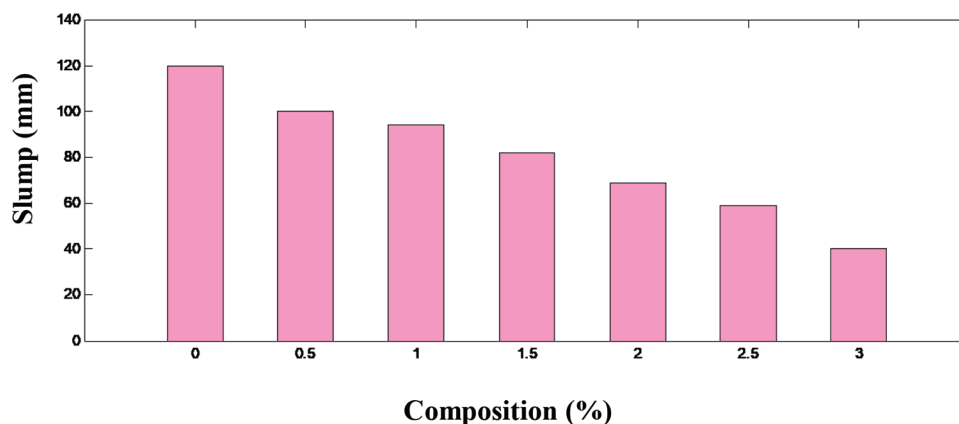


Fig. 3—Slump values of concrete with varying NT percentage.

uneven shape of the material enhance interlocking and hardness, hence minimizing the ball-bearing effect.⁴⁴ As a result of all of these factors, concrete containing NT has a lower slump and a higher water requirement. When the slump test results were compared to those from earlier research,^{45,46} it was determined that there was a high degree of agreement that increasing NT decreased slump value.^{3,5,10}

Although the addition of TiO_2 nanoparticles in various volume fractions reduced flowability characteristics, the nanoparticles increased the consistency of the concrete mixtures.⁴⁷ In the mixtures containing TiO_2 nanoparticles, there was less bleeding and segregation.

Mechanical properties

Figures 4 to 6 show the compressive, splitting tensile, and flexural strength of each combination as an average of three specimens at 7, 28, 56, and 90 days. At 7 days of age, NT0's compressive strength was tested to be 3237.24 psi (22.32 MPa). When NT0.5, NT1, and NT1.5 were compared to the control mixture (that is, NT0), the compressive strength increased nominally by 2.15%, 5.15%, and 18.67%, respectively. The percentage increase in strength of NT2 and NT2.5 was determined to be 6.67% and 3.34%, respectively. The maximum gain in compressive strength was found at a replacement level of 1.5%.

As shown in Fig. 5, splitting tensile strength was tested with NT substitution in various percentages. The splitting tensile strength of the NT1, NT1.5, and NT2 concrete mixtures increased on all days when compared to the control mixture. On the 28th day, the splitting tensile strength improved significantly when compared to the seventh day. When 1.5% of the cement in concrete was substituted with NT, the splitting tensile strength rose.

The effect of nominal pozzolanic activity of NT and the filler effect could be some of the probable explanations for the improvement in strength up to 1.5% of NT. The type of cement paste produced and the interfacial transition zone (ITZ), both of which affect tensile strength, are also influenced by NT properties. At 7 days, the splitting tensile strength of NT0 was 2.2 MPa, whereas the splitting tensile strength of the other mixtures NT0.5, NT1.0, NT1.5, NT2, NT2.5, and NT3 were 333.58 psi (2.3 MPa), 362.59 (2.5 MPa),

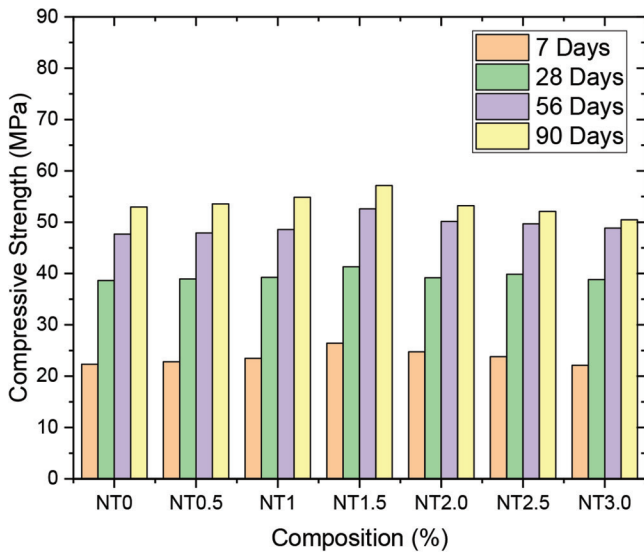


Fig. 4—Compressive strength of concrete containing NT.

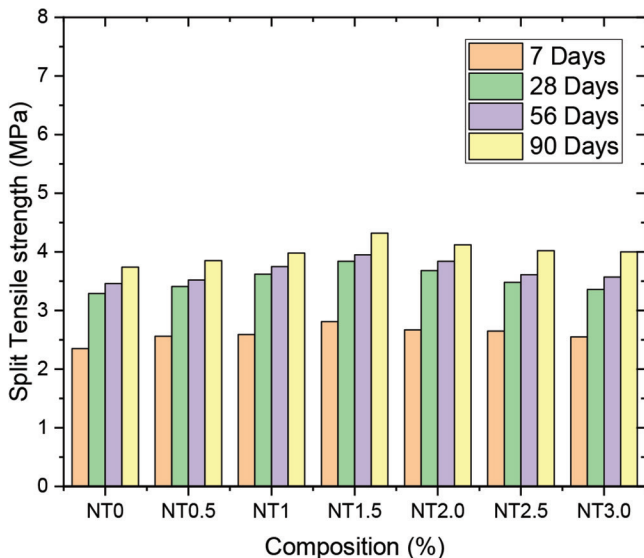


Fig. 5—Splitting tensile strength concrete containing NT.

406.10 psi (2.8 MPa), 390.15 psi (2.69 MPa), 384.35 psi (2.65 MPa), and 359.69 psi (2.48 MPa), respectively.

The beam flexural strength after 7, 28, 56, and 90 days is shown in Fig. 6. The strength parameters are comparable to those of splitting tensile strength, with low strength at 7 days and a significant increase at 28 days.

At 56 and 90 days, a minor increase in strength is also observed while the hydration process continues. At 1.5% replacement, flexural strength, like compressive and splitting tensile strength, reaches a maximum value.

Sorptivity

All samples were tested for capillary suction after curing for 28 days using a sorptivity test. Sorptivity is the slope of the straight line that displays the relationship between absorption and the square root of time.^{7,29} In Table 8, the absorption as a function of time and the square root of the absorption coefficient are presented for the NT concrete mixtures.²¹ The concrete mixtures with NT3.0 have the lowest sorptivity, followed by NT2.5, NT2, NT1.5, NT1,

Table 8—Sorptivity and water absorption of concrete containing NT

NT, %	Sorptivity, mm/sec ^{0.5}	Water absorption, %	Apparent porosity, %
NT	0.0477	4.96	25.45
NT0.5	0.0409	4.89	23.62
NT1.0	0.0359	4.74	21.65
NT1.5	0.0369	4.64	19.27
NT2.0	0.0327	4.59	16.31
NT2.5	0.0231	4.45	14.08
NT3.0	0.0102	4.36	10.63

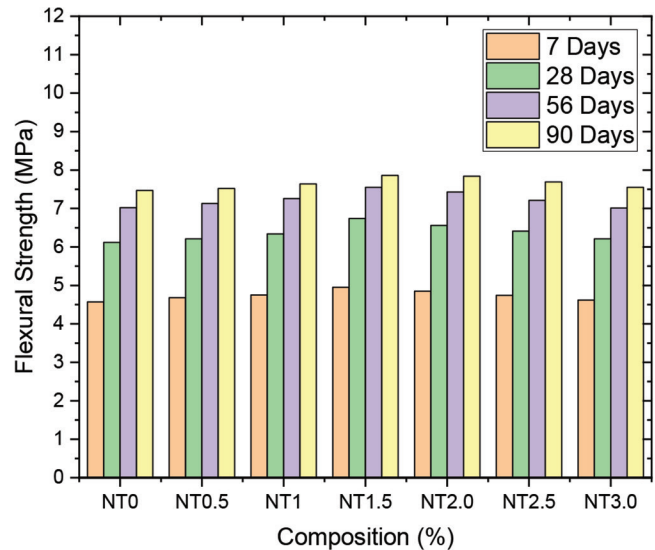


Fig. 6—Flexural strength of concrete containing NT.

NT0.5, and NT0. Pore characteristics can be related to differences in sorptivity levels.

The smaller particle size of NT results in the low sorptivity, and increasing the production of calcium-silicate-hydrate (C-S-H) gel shrinks the pores, hence decreasing the sorptivity.⁴ Due to the presence of NT in the C-S-H gel, samples containing a higher concentration of NT demonstrated lower sorptivity.^{48,49} As a result, the pores become less connected, resulting in decreased absorption.³⁸ These findings are consistent with those reported in previous research on water absorption (Table 8).

Water absorption

Water absorption was determined using soaking tests, and the findings are reported in Table 8. Water absorption increased throughout 24 hours. Water absorption reduced as the fraction of NT increased, owing to the increase in smaller particles.²⁵ This is in addition to the results obtained for sorptivity and apparent porosity. Sorptivity and apparent porosity diminish when the NT content increases.

Apparent porosity

Three cubes from each series were oven-dried for 24 hours at 185°F (85°C) to determine the water absorption capacity of mortar specimens, and their weight served as the starting

weight. After 24 hours of immersion in water, the saturated surface-dry weight of the samples was determined to be the final weight. The weight loss of specimens that have absorbed water is expressed as a percentage.⁴⁶ The specimens were dried at 185°F (85°C) because higher temperatures could disturb the microstructure of mortar specimens, resulting in erroneous water absorption measurements.^{50,51} The third set of three samples was used to determine the apparent porosity.

The following equation was used to find the apparent porosity

$$\text{Apparent porosity} = [(M_w - M_d)/(M_w - NT)] \times 100\%$$

where M_w is the weight of the specimen after immersion in water for 48 hours; M_d is the weight of the specimen after oven drying at 185°F (85°C) for 24 hours; and NT is the weight of the specimen suspended in water.

UPV and dynamic modulus of elasticity

The UPV test is a nondestructive technique for measuring the dynamic modulus of elasticity of concrete specimens as well as their quality and homogeneity.⁵² Additionally, this test can be used to discover concrete fractures, defects, and pores. In the current investigation, concrete cube samples cast for compressive strength were subjected to a UPV test before being evaluated for compression on the 28th day. After coating the test surface with petroleum jelly to ensure good acoustic coupling, the pulse velocity was applied through the direct transmission method.⁵³ The variability of the results for each specimen was reduced by dividing the cube surface into three 3 x 3 grids, as the test is dependent on a variety of variables, including aggregate density and modulus; physical and mechanical properties of cement; the presence of voids; moisture; temperature; and the mixture, shape, and size of concrete.¹⁵ UPV measurements were obtained and averaged at each junction location. The wave velocity was calculated using Erdogan's proposed equation³¹

$$V = (h/t) \times 10^6$$

where V is the ultrasonic wave speed (m/s); h is the distance between the surface of the concrete specimen from which the ultrasonic wave is sent and the surface where the wave is received (m); and t is the time passed from the concrete surface from which the ultrasonic wave is sent and the surface wave is received (μ s).

The UPV of concrete containing varying concentrations of NT after 28 days is illustrated in Table 9. In general, when the NT content increases, the UPV values fall. However, all concrete containing NT falls within the category of good concrete, as defined by IS 13311-2:1992,⁵³ with UPV values of more than 5000 m/s. Additionally, all concrete can be regarded as being of high-quality NT of uniformity and integrity.⁵⁴ As a result, it can be inferred that the addition of NT to concrete improves its UPV testing quality. The decrease in voids and microcracks observed as the NT concentration increased could be attributed to NT filler action, which lowers voids and microcracks.⁴³

Table 9—UPV at 28 days

S. No.	Mixture	UPV, m/s
1	NT0	6173.44
2	NT0.5	6126.42
3	NT1.0	6052.05
4	NT1.5	5918.63
5	NT2.0	5812.55
6	NT2.5	5699.91
7	NT3.0	5602.58

Işıkdağ and Topçu⁵⁵ provided formulas for calculating the dynamic modulus of elasticity (E_d). The formula is as follows

$$E_d = V^2 \gamma (1 + \mu)(1 - 2\mu) \times 10^{-6} / (1 - \mu)$$

where μ is the dynamic Poisson's ratio for concrete and is taken as 0.23; and γ is the unit weight (kg/m^3).

Figure 7 shows the dynamic modulus of elasticity in GPa versus the percentage of NT.

Chloride penetration

Cubic specimens 150 x 150 x 150 mm were immersed in a 3% NaCl solution for 90 days after a 90-day curing period. Then specimens were oven-dried for 24 hours. After that, to prepare some pulverized concrete samples (powder samples) for the test, all six faces of the cubic specimens were drilled to depths of 0 to 0.19 in. (0 to 5 mm), 0.19 to 0.39 in. (5 to 10 mm), 0.39 to 0.59 in. (10 to 15 mm), 0.59 to 0.78 in. (15 to 20 mm), and 0.78 to 1.81 in. (20 to 30 mm). The concrete powder samples obtained from all six faces for each depth were blended, and the samples were ready for the next step of the test (ASTM C1218/C1218M-15).⁵⁶

The total chloride content of pulverized concrete is determined using a potentiometric titration of chloride with silver nitrate (ASTM C114)⁵⁷ in this test procedure. The produced crushed concrete sample is dissolved in nitric acid, and if the solution is acidic, a small amount of NaHCO_3 is added until the pH value reaches 6 or 7. The K_2CrO_4 indicator is then added, resulting in a light yellow color change in the solution. Eventually, 0.05 N AgNO_3 is added until the solution turns orange-yellow (weak brown) in color, and the volume of the AgNO_3 solution is measured. To determine the Cl ion percentage, the volume of the AgNO_3 solution is substituted in the following equation

$$\text{Cl}^- (\%) = \frac{3.5453(V \cdot N)}{W}$$

where W is the weight of pulverized (powder) concrete prepared from the sample; N is the normality of AgNO_3 solution; and V is the volume of AgNO_3 solution.

In this study, the chloride penetration was calculated as a fraction of the weight of the concrete sample.⁵⁸ The chloride percentages at various depths of the concrete samples are shown in Fig. 8.

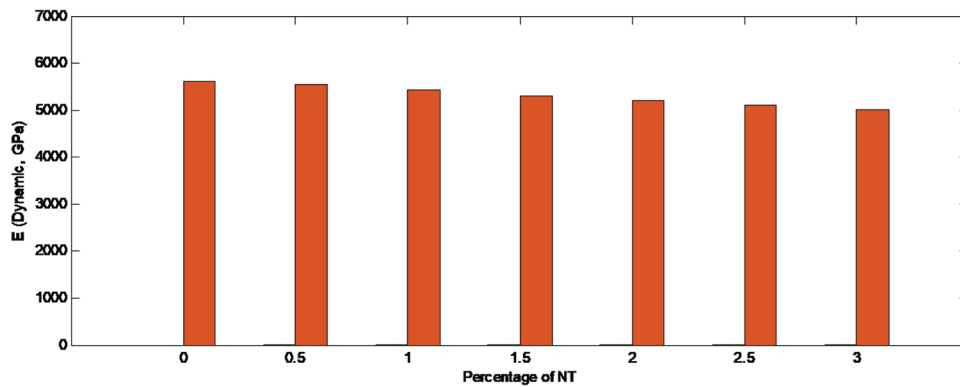


Fig. 7—Dynamic modulus of elasticity (GPa) versus percentage of NT.

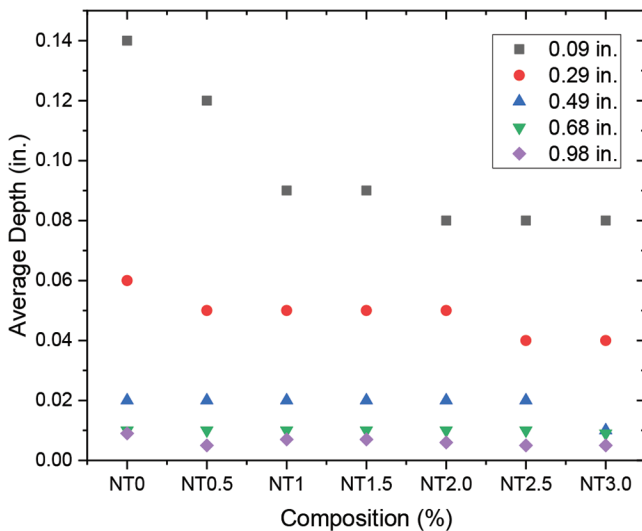


Fig. 8—Chloride penetration depth versus percentage of NT.

The results show a general decrease in chloride percentage by the depth of the concrete sample, indicating that the concrete components, particularly aggregates, are free of chloride ions.

According to the results obtained, increasing the TiO_2 nanoparticles to a concentration of 3 wt. % results in a decrease in chloride penetration. The findings of this study corroborate those of other researchers.^{58,59} For instance, Detwiler et al.¹ investigated the efficacy of using supplementary cementitious materials to improve the chloride resistance of accelerated cured concrete and discovered that concretes containing supplementary cementitious materials outperformed portland cement concrete. Additionally, the use of supplementary cementitious materials can help prevent detrimental expansions caused by both delayed ettringite formation and the alkali-silica reaction.⁶⁰

Regarding the beneficial effect of TiO_2 nanoparticles as supplementary cementitious materials on chloride penetration through concrete, this could be because the nanoparticles located in the cement paste as the kernel can further promote cement hydration due to their high activity, resulting in a more homogeneous and compact cement paste.⁵⁸ As a result, the pore structure of concrete is significantly improved. When the nanoparticle content is increased above 3% by weight, the improvement in the pore structure of concrete is weakened.⁶⁰ This is because the distance

between nanoparticles decreases as the nanoparticle content increases, and the $\text{Ca}(\text{OH})_2$ crystal quantity decreases as a result.⁶¹ This results in a low ratio of crystal to strengthening gel, increased shrinkage and creep of the cement matrix, and a looser pore structure of the cement matrix, which could result in increased chloride penetration.⁵¹

Figure 8 shows the percentage of chloride penetration at different average depths of the concrete samples.

MICROSTRUCTURE

The SEM images at 50 μm magnification for all the samples are presented in Fig. 9. While the matrix of the control mixture and 1% NT showed relatively larger (approximately 10 μm) pores unevenly distributed, the 2% NT showed smaller-sized pores (approximately 2 to 3 μm) more uniformly distributed, and 3% NT showed relatively lesser pores. The 2% NT and 3% NT also exhibited the formation of more C-S-H gel. Thus, it is inferred that the higher the percentage of NT, the lesser the pores.

SEM aids in the characterization of concrete's microstructure and the identification of the components that affect its mechanical properties and durability.⁶² The concrete microstructure is made up of C-S-H gel, calcium hydroxide, calcium sulfoaluminate hydrate (ettringite and monosulfate), coarse and fine aggregate, and an ITZ between the aggregate and cement hydration products. In EDS spot analysis results, calcium, silica, and alumina content in NT were discovered in percentages of 35.24, 29.3, and 12.87, respectively. Figures 9(a) and (b) show the microstructure of NT0 and NT1.0 concrete.

The microstructure of the specimens changed after 28 days of curing in all of the replacements. The main hydration product, C-S-H gel, which was responsible for improved mechanical properties, is present in significant quantity. Hence, a sharp rise in the value of strength parameters was observed at 28 days. A pozzolanic reaction and the production of a C-S-H gel were observed after 28 days of curing. Figure 9 shows the microstructure of NAC, NT1.0, NT2, and NT3 at 50 μm magnification. Figure 9(a) shows the microstructure of the control mixture. Micropores up to 5 μm are seen scattered along with the matrix. NT1.0 (Fig. 9(b)) and NT2 (Fig. 9(c)) show a progressively improving microstructure with smaller voids and less in number. The ITZ is intact, as seen in NT2 (Fig. 9(c)). In the case of NT3 (Fig. 9(d)), EDS spot analysis revealed a

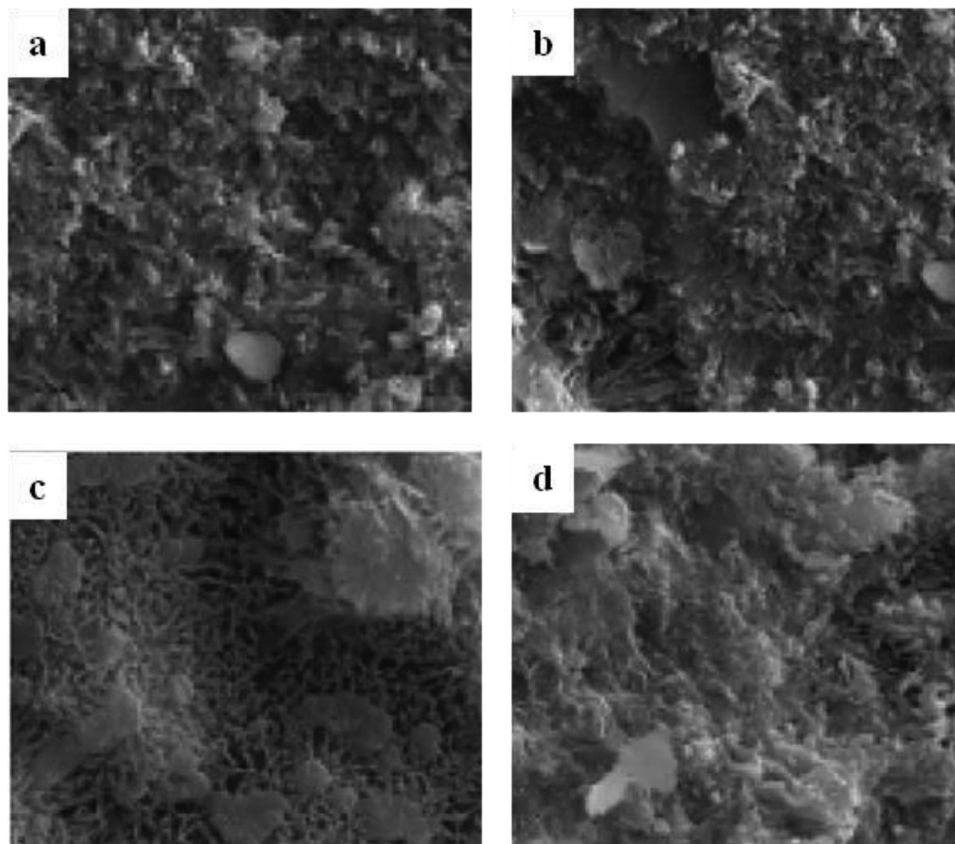


Fig. 9—Microstructure of mortar containing: (a) control mixture; (b) 1% NT; (c) 2% NT; and (d) 3% NT.

dense microstructure and minimal voids. This is consistent with the findings of compressive strength and further establishes the two-wall effect. The aggregates of NT3 are well covered with the matrix and exhibit an excellent bond with the matrix. Microcracks and micropores are nearly absent in this sample.¹ The presence of NT thus reduces the voids in the concrete.

CONCLUSIONS

Experimental investigations to study the effect of partial replacement of cement with nano-titanium dioxide (nano-TiO₂ [NT]) are attempted in this research work. The physical and chemical properties of NT and its viability to be used as a replacement for cement are studied. The results obtained in this study can be summarized as follows:

- Increases in the fraction of nanoparticles often enhanced the durability of the resulting concrete, which might be attributed to finer particles in the cement mixture and the nanoparticles' filler effect.
- TiO₂ nanoparticles as a partial replacement for cement up to 1.5% could accelerate the formation of calcium-silicate-hydrate (C-S-H) gels due to increased crystalline Ca(OH)₂ concentration at an early stage of hydration, thereby increasing the flexural and splitting tensile strengths of concrete specimens even at early stages of hydration. The presence of more than 1.5% of TiO₂ nanoparticles results in decreased flexural and splitting tensile strengths because of the decreased crystalline Ca(OH)₂ content necessary for C-S-H gel formation.

- Both water absorption and apparent porosity were significantly reduced with the addition of TiO₂ nanoparticles, as the nanoparticles act as nanofillers and improve the concrete resistance to water permeability.
- Ultrasonic pulse velocity (UPV) tests revealed that when TiO₂ nanoparticles are added, the number of pores in the concrete decreases, indicating that the density of the concrete is raised and the pore structure is improved.
- Chloride penetration decreased with the inclusion of nanoparticles, which could be due to the more packed microstructure created by the nanoparticles and the increased volume of the paste.

AUTHOR BIOS

Garima Rawat is a PhD Scholar at Jaypee University of Engineering and Technology, Guna, Madhya Pradesh, India, where she received her BTech and MTech in civil engineering in 2015 and 2017, respectively. Her research interests include the cathodic protection of marine structures, strength and durability properties of structures, and chloride diffusivity in concrete structures.

Sumit Gandhi is an Associate Professor and Head. He received his BTech in civil engineering from Kavayitri Bahinabai Chaudhari North Maharashtra University, Jalgaon, Maharashtra, India, in 2001; his MTech in water resource engineering from Motilal Nehru National Institute of Technology Allahabad, Prayagraj, Uttar Pradesh, India, in 2004; and his PhD from Motilal Nehru National Institute of Technology Allahabad in 2009. His area of work during his PhD was flow behavior in prismatic and nonprismatic open channels. He has extensive teaching and research experience in the field of civil engineering.

Yogesh Iyer Murthy received his BE in civil engineering from Dayananda Sagar College of Engineering, Bengaluru, Karnataka, India, in 2002, with honors; his ME in structural engineering from Shri Govindram Seksaria Institute of Technology and Science, Indore, Madhya Pradesh, India, in 2010; and his PhD from Jaypee University of Engineering and Technology

in 2021. His ME thesis was on the transient dynamics of laminated fiber-reinforced composite plates using quadrilateral flat-facet shell elements, and the focus of his PhD work was on corrosion mitigation of structures using magnesium alloys as sacrificial anodes.

REFERENCES

1. Detwiler, R. J.; Fapohunda, C. A.; and Natale, J., "Use of Supplementary Cementing Materials to Increase the Resistance to Chloride Ion Penetration of Concretes Cured at Elevated Temperatures," *ACI Materials Journal*, V. 91, No. 1, Jan-Feb. 1994, pp. 63-66.
2. Luna, F. J.; Fernández, A.; and Alonso, M. C., "The Influence of Curing and Aging on Chloride Transport through Ternary Blended Cement Concrete," *Materiales de Construcción*, V. 68, No. 332, Oct.-Dec. 2018, Article No. e171. doi: 10.3989/mc.2018.11917
3. Saloma; Nasution, A.; Imran, I.; and Abdullah, M., "Improvement of Concrete Durability by Nanomaterials," *Procedia Engineering*, V. 125, 2015, pp. 608-612. doi: 10.1016/j.proeng.2015.11.078
4. Jayapalan, A. R.; Lee, B. Y.; and Kurtis, K. E., "Effect of Nano-sized Titanium Dioxide on Early Age Hydration of Portland Cement," *Nanotechnology in Construction: Proceedings of the NICOM3*, Z. Bittnar, P. J. M. Bartos, J. Němeček, V. Šmilauer, and J. Zeman, eds., Springer-Verlag, Berlin, Germany, 2009, pp. 267-273. doi: 10.1007/978-3-642-00980-8_35
5. Du, S.; Wu, J.; AlShareedah, O.; and Shi, X., "Nanotechnology in Cement-Based Materials: A Review of Durability, Modeling, and Advanced Characterization," *Nanomaterials (Basel)*, V. 9, No. 9, Sept. 2019, Article No. 1213. doi: 10.3390/nano9091213
6. Khataee, R.; Heydari, V.; Moradkhannejhad, L.; Safarpour, M.; and Joo, S. W., "Self-Cleaning and Mechanical Properties of Modified White Cement with Nanostructured TiO₂," *Journal of Nanoscience and Nanotechnology*, V. 13, No. 7, July 2013, pp. 5109-5114. doi: 10.1166/jnn.2013.7586
7. Nazari, A., "The Effects of Curing Medium on Flexural Strength and Water Permeability of Concrete Incorporating TiO₂ Nanoparticles," *Materials and Structures*, V. 54, No. 4, 2021, Article No. 174.
8. Nazari, A., and Riahi, S., "TiO₂ Nanoparticles' Effects on Properties of Concrete Using Ground Granulated Blast Furnace Slag as Binder," *Science China Technological Sciences*, V. 64, No. 9, Sept. 2021, p. 2066.
9. Wang, L.; Zhang, H.; and Gao, Y., "Effect of TiO₂ Nanoparticles on Physical and Mechanical Properties of Cement at Low Temperatures," *Advances in Materials Science and Engineering*, V. 2018, 2018, 12 pp. doi: 10.1155/2018/8934689
10. Shekari, A. H., and Razzaghi, M. S., "Influence of Nano Particles on Durability and Mechanical Properties of High Performance Concrete," *Procedia Engineering*, V. 14, 2011, pp. 3036-3041. doi: 10.1016/j.proeng.2011.07.382
11. Shen, W.; Zhang, C.; Li, Q.; Zhang, W.; Cao, L.; and Ye, J., "Preparation of Titanium Dioxide Nano Particle Modified Photocatalytic Self-Cleaning Concrete," *Journal of Cleaner Production*, V. 87, Jan. 2015, pp. 762-765. doi: 10.1016/j.jclepro.2014.10.014
12. Abdalla, J. A.; Thomas, B. S.; Hawileh, R. A.; Yang, J.; Jindal, B. B.; and Ariyachandra, E., "Influence of Nano-TiO₂, Nano-Fe₂O₃, Nanoclay and Nano-CaCO₃ on the Properties of Cement/Geopolymer Concrete," *Cleaner Materials*, V. 4, June 2022, Article No. 100061. doi: 10.1016/j.clema.2022.100061
13. Han, B.; Sun, S.; Ding, S.; Zhang, L.; Yu, X.; and Ou, J., "Review of Nanocarbon-Engineered Multifunctional Cementitious Composites," *Composites Part A: Applied Science and Manufacturing*, V. 70, Mar. 2015, pp. 69-81. doi: 10.1016/j.compositesa.2014.12.002
14. Vittoriadimanti, M., and Pedferri, M. P., "Concrete, Mortar and Plaster Using Titanium Dioxide Nanoparticles: Applications in Pollution Control, Self-Cleaning and Photo Sterilization," *Nanotechnology in Eco-Efficient Construction: Materials, Processes and Applications*, F. Pacheco-Torgal, M. V. Diamanti, A. Nazari, and C-G. Granqvist, eds., Woodhead Publishing, Sawston, UK, 2013, pp. 299-326. doi: 10.1533/9780857098832.3.299
15. Lee, B. Y., "Effect of Titanium Dioxide Nanoparticles on Early Age and Long Term Properties of Cementitious Materials," PhD dissertation, Georgia Institute of Technology, Atlanta, GA, Aug. 2012, 227 pp.
16. Meng, T.; Yu, Y.; Qian, X.; Zhan, S.; and Qian, K., "Effect of Nano-TiO₂ on the Mechanical Properties of Cement Mortar," *Construction and Building Materials*, V. 29, Apr. 2012, pp. 241-245. doi: 10.1016/j.conbuildmat.2011.10.047
17. Mohammadi, M.; Hesaraki, S.; and Hafezi-Ardakani, M., "Investigation of Biocompatible Nanosized Materials for Development of Strong Calcium Phosphate Bone Cement: Comparison of Nano-Titania, Nano-Silicon Carbide and Amorphous Nano-Silica," *Ceramics International*, V. 40, No. 6, July 2014, pp. 8377-8387. doi: 10.1016/j.ceramint.2014.01.044
18. Raki, L.; Beaudoin, J.; Alizadeh, R.; Makar, J.; and Sato, T., "Cement and Concrete Nanoscience and Nanotechnology," *Materials (Basel)*, V. 3, No. 2, 2010, pp. 918-942. doi: 10.3390/ma3020918
19. Senff, L.; Tobaldi, D. M.; Lucas, S.; Hotza, D.; Ferreira, V. M.; and Labrincha, J. A., "Formulation of Mortars with Nano-SiO₂ and Nano-TiO₂ for Degradation of Pollutants in Buildings," *Composites Part B: Engineering*, V. 44, No. 1, Jan. 2013, pp. 40-47. doi: 10.1016/j.compositesb.2012.07.022
20. Lazaro, A.; Yu, Q. L.; and Brouwers, H. J. H., "Nanotechnologies for Sustainable Construction," *Sustainability of Construction Materials*, second edition, J. M. Khatib, ed., Woodhead Publishing, Sawston, UK, 2016, pp. 55-78. doi: 10.1016/b978-0-08-100370-1.00004-4
21. Chen, J.; Kou, S.-C.; and Poon, C.-S., "Hydration and Properties of Nano-TiO₂ Blended Cement Composites," *Cement and Concrete Composites*, V. 34, No. 5, May 2012, pp. 642-649. doi: 10.1016/j.cemconcomp.2012.02.009
22. Nazar, S.; Yang, J.; Thomas, B. S.; Azim, I.; and Ur Rehman, S. K., "Rheological Properties of Cementitious Composites with and without Nano-Materials: A Comprehensive Review," *Journal of Cleaner Production*, V. 272, Nov. 2020, Article No. 122701. doi: 10.1016/j.jclepro.2020.122701
23. Yan, D.; Wu, C.; Lin, Z.; Leventis, N.; and Mahadik, S., "Concrete Surface with Nano-Particle Additives for Improved Wearing Resistance to Increasing Truck Traffic," Report No. MATC-MST: 441, Mid-America Transportation Center, Lincoln, NE, 2012, 53 pp.
24. Noorvand, H.; Abang Ali, A. A.; Demirboga, R.; Farzadnia, N.; and Noorvand, H., "Incorporation of Nano TiO₂ in Black Rice Husk Ash Mortars," *Construction and Building Materials*, V. 47, Oct. 2013, pp. 1350-1361. doi: 10.1016/j.conbuildmat.2013.06.066
25. IS 2386-1963(R2016), "Methods of Test for Aggregates for Concrete (Part I to Part VIII) (Revision 2016)," Bureau of Indian Standards, New Delhi, India, 2016.
26. IS 516-1959(R2004), "Method of Tests for Strength of Concrete (Reaffirmed 2004)," Bureau of Indian Standards, New Delhi, India, 2004, 30 pp.
27. Lucas, S. S.; Ferreira, V. M.; and Barroso de Aguiar, J. L., "Incorporation of Titanium Dioxide Nanoparticles in Mortars – Influence of Microstructure in the Hardened State Properties and Photocatalytic Activity," *Cement and Concrete Research*, V. 43, Jan. 2013, pp. 112-120. doi: 10.1016/j.cemconres.2012.09.007
28. Konsta-Gdoutos, M. S.; Metaxa, Z. S.; and Shah, S. P., "Highly Dispersed Carbon Nanotube Reinforced Cement Based Materials," *Cement and Concrete Research*, V. 40, No. 7, July 2010, pp. 1052-1059. doi: 10.1016/j.cemconres.2010.02.015
29. Saleem, H.; Zaidi, S. J.; and Alnuaimi, N. A., "Recent Advancements in the Nanomaterial Application in Concrete and Its Ecological Impact," *Materials (Basel)*, V. 14, No. 21, Nov. 2021, Article No. 6387. doi: 10.3390/ma14216387
30. Yu, X.; Kang, S.; and Long, X., "Compressive Strength of Concrete Reinforced by TiO₂ Nanoparticles," *AIP Conference Proceedings*, V. 2036, No. 1, 2018, Article No. 030006. doi: 10.1063/1.5075659
31. Jalal, M., "Durability Enhancement of Concrete by Incorporating Titanium Dioxide Nanopowder into Binder," *The Journal of American Science*, V. 8, No. 4, 2012, pp. 289-294.
32. Mulenga, D. M., and Robery, P. C., "Can Nanotechnology Address Today's Civil Engineering Challenges?" *Structures Congress 2010*, S. Senapathi, K. Casey, and M. Hoit, eds., Orlando, FL, 2010, pp. 609-621. doi: 10.1061/41130(369)5610.1061/41130(369)56
33. Du, Y.; Yang, J.; Skariah Thomas, B.; Li, L.; Li, H.; Mohamed Shaban, W.; and Tung Chong, W., "Influence of Hybrid Graphene Oxide/Carbon Nanotubes on the Mechanical Properties and Microstructure of Magnesium Potassium Phosphate Cement Paste," *Construction and Building Materials*, V. 260, Nov. 2020, Article No. 120449. doi: 10.1016/j.conbuildmat.2020.120449
34. IS 12269:2013, "Ordinary Portland Cement, 53 Grade — Specification (First Revision)," Bureau of Indian Standards, New Delhi, India, 2013, 14 pp.
35. IS 383-2016, "Specification for Coarse and Fine Aggregates from Natural Sources for Concrete," Bureau of Indian Standards, New Delhi, India, 2016, 24 pp.
36. IS 456:2000, "Plain and Reinforced Concrete — Code of Practice (Fourth Revision) (Reaffirmed 2005)," Bureau of Indian Standards, New Delhi, India, 2000, 114 pp.
37. IS 10500:2012, "Drinking Water — Specification (Second Revision)," Bureau of Indian Standards, New Delhi, India, 2012, 18 pp.
38. IS 10262:2019, "Concrete Mix Proportioning — Guidelines (Second Revision)," Bureau of Indian Standards, New Delhi, India, 2019, 21 pp.
39. IS 1199-1959, "Methods of Sampling and Analysis of Concrete (Reaffirmed 2004)," Bureau of Indian Standards, New Delhi, India, 1959, 49 pp.

40. IS 5816:1999, "Splitting Tensile Strength of Concrete — Method of Test (Reaffirmed 2004)," Bureau of Indian Standards, New Delhi, India, 1999, 14 pp.
41. Salman, M. M.; Eweed, K. M.; and Hameed, A. M., "Influence of Partial Replacement TiO₂ Nanoparticles on the Compressive and Flexural Strength of Ordinary Cement Mortar," *Al-Nahrain University, College of Engineering Journal (NUCEJ)*, V. 19, No. 2, 2016, pp. 265-270.
42. Ur Rehman, A.; Qudoos, A.; Kim, H. G.; and Ryou, J.-S., "Influence of Titanium Dioxide Nanoparticles on the Sulfate Attack upon Ordinary Portland Cement and Slag-Blended Mortars," *Materials (Basel)*, V. 11, No. 3, Mar. 2018, Article No. 356. doi: 10.1016/j.enbuild.2010.12.025
43. Feng, D.; Xie, N.; Gong, C.; Leng, Z.; Xiao, H.; Li, H.; and Shi, X., "Portland Cement Paste Modified by TiO₂ Nanoparticles: A Microstructure Perspective," *Industrial & Engineering Chemistry Research*, V. 52, No. 33, Aug. 2013, pp. 11575-11582. doi: 10.1021/ie4011595
44. Essawy, A. A., and Abd El.Aleem, S., "Physico-Mechanical Properties, Potent Adsorptive and Photocatalytic Efficacies of Sulfate Resisting Cement Blends Containing Micro Silica and Nano-TiO₂," *Construction and Building Materials*, V. 52, Feb. 2014, pp. 1-8. doi: 10.1016/j.conbuildmat.2013.11.026
45. Isfahani, F. T.; Redaelli, E.; Lollini, F.; Li, W.; and Bertolini, L., "Effects of Nanosilica on Compressive Strength and Durability Properties of Concrete with Different Water to Binder Ratios," *Advances in Materials Science and Engineering*, V. 2016, 2016, 16 pp. doi: 10.1155/2016/8453567
46. Nazari, A., and Riahi, S., "The Effect of TiO₂ Nanoparticles on Water Permeability and Thermal and Mechanical Properties of High Strength Self-Compacting Concrete," *Materials Science and Engineering: A*, V. 528, No. 2, Dec. 2010, pp. 756-763. doi: 10.1016/j.msea.2010.09.074
47. Soleymani, F., "Assessments of the Effects of Limewater on Water Permeability of TiO₂ Nanoparticles Binary Blended Palm Oil Clinker Aggregate-Based Concrete," *The Journal of American Science*, V. 8, No. 5, 2012, pp. 698-702.
48. Zhang, R.; Cheng, X.; Hou, P.; and Ye, Z., "Influences of Nano-TiO₂ on the Properties of Cement-Based Materials: Hydration and Drying Shrinkage," *Construction and Building Materials*, V. 81, Apr. 2015, pp. 35-41. doi: 10.1016/j.conbuildmat.2015.02.003
49. Iyappan, A. P.; Srikanthan, L.; Franklin, F. S.; Bhuvanawari, J.; and Preethika, A., "Replacement of Cement by Using Nano Titanium Dioxide in Concrete," *IJSRD-International Journal for Scientific Research & Development*, V. 5, No. 7, 2017, pp. 499-503.
50. Zhao, L.; Chen, R.; Pang, L. X.; Zhang, W.; and Tan, X., "Study on Photo-Catalytic Efficiency and Durability of Nano-TiO₂ in Permeable Concrete Pavement Structure," *IOP Conference Series: Earth and Environmental Science*, V. 371, No. 4, 2019, Article No. 042011. doi: 10.1088/1755-1315/371/4/042011
51. Zhang, M.-H., and Li, H., "Pore Structure and Chloride Permeability of Concrete Containing Nano-Particles for Pavement," *Construction and Building Materials*, V. 25, No. 2, Feb. 2011, pp. 608-616. doi: 10.1016/j.conbuildmat.2010.07.032
52. Bleszynski, R.; Hooton, R. D.; Thomas, M. D. A.; and Rogers, C. A., "Durability of Ternary Blend Concrete with Silica Fume and Blast-Furnace Slag: Laboratory and Outdoor Exposure Site Studies," *ACI Materials Journal*, V. 99, No. 5, Sept.-Oct. 2002, pp. 499-508.
53. IS 13311-2:1992, "Non-Destructive Testing of Concrete — Methods of Test: Part 2: Rebound Hammer (Reaffirmed 2004)," Bureau of Indian Standards, New Delhi, India, 1992, 12 pp.
54. Senff, L.; Hotza, D.; Lucas, S.; Ferreira, V. M.; and Labrincha, J. A., "Effect of Nano-SiO₂ and Nano-TiO₂ Addition on the Rheological Behavior and the Hardened Properties of Cement Mortars," *Materials Science and Engineering: A*, V. 532, Jan. 2012, pp. 354-361. doi: 10.1016/j.msea.2011.10.102
55. Işıkdag, B., and Topçu, İ. B., "The Effect of Ground Granulated Blast-Furnace Slag on Properties of Horasan Mortar," *Construction and Building Materials*, V. 40, Mar. 2013, pp. 448-454. doi: 10.1016/j.conbuildmat.2012.11.016
56. ASTM C1218/C1218M-15, "Standard Test Method for Water-Soluble Chloride in Mortar and Concrete," ASTM International, West Conshohocken, PA, 2015, 3 pp.
57. Bouchard, B., "ASTM C-114 Accreditation for Cement Analysis by Fusion," SPEX SamplePrep, Metuchen, NJ.
58. Bassuoni, M. T.; Nehdi, M. L.; and Greenough, T. R., "Enhancing the Reliability of Evaluating Chloride Ingress in Concrete Using the ASTM C 1202 Rapid Chloride Penetrability Test," *Journal of ASTM International*, V. 3, No. 3, 2006, 13 pp. doi: 10.1520/jai13403
59. Ribeiro, D. V.; Labrincha, J. A.; and Morelli, M. R., "Chloride Diffusivity in Red Mud-Ordinary Portland Cement Concrete Determined by Migration Tests," *Materials Research*, V. 14, No. 2, 2011, pp. 227-234. doi: 10.1590/S1516-14392011005000026
60. Gailius, A., and Kosior-Kazberuk, M., "Monitoring of Concrete Resistance to Chloride Penetration," *Materials Science (Medžiagotyra)*, V. 14, No. 4, 2008, pp. 350-355.
61. Özyurt, N.; Söylev, T. A.; Özturan, T.; Pehlivan, A. O.; and Niş, A., "Corrosion and Chloride Diffusivity of Reinforced Concrete Cracked under Sustained Flexure," *Teknik Dergi*, V. 31, No. 6, 2020, pp. 10315-10337. doi: 10.18400/teker.430536
62. Ramirez-Meneses, E.; Dominguez-Crespo, M. A.; and Torres-Huerta, A. M., "Stabilized Metal Nanoparticles from Organometallic Precursors for Low Temperature Fuel Cells," *Recent Patents on Nanotechnology*, V. 7, No. 1, 2012, pp. 13-25. doi: 10.2174/1872210511307010013

NOTES:
